

The distribution of current helicity at the solar surface at the beginning of the solar cycle

D. Sokoloff^{1,6,*}, S.D. Bao¹, N. Kleeorin², K. Kuzanyan^{3,4}, D. Moss⁵, I. Rogachevskii², D. Tomin⁷, and H. Zhang¹

¹ National Astronomical Observatories, Chinese Academy of Sciences, Beijing 100012, China

² Department of Mechanical Engineering, Ben-Gurion University of Negev, POB 653, 84105 Beer-Sheva, Israel

³ IZMIRAN, Troitsk, Moscow Region 142190, Russia

⁴ School of Mathematics, University of Leeds, Leeds LS2 9JT, UK

⁵ School of Mathematics, University of Manchester, Manchester M13 9PL, UK

⁶ Department of Physics, Moscow State University, Moscow 119992, Russia

⁷ Department of Mechanics and Mathematics, Moscow State University, Moscow 119992, Russia

Received 2006 Mar 09, accepted 2006 Jun 18

Published online 2006 Oct 16

Key words Sun: magnetic fields

A fraction of solar active regions are observed to have current helicity of a sign that contradicts the polarity law for magnetic helicity; this law corresponds to the well-known polarity law for sunspots. A significant excess of active regions with the “wrong” sign of helicity is seen to occur just at the beginning of the cycle. We compare these observations with predictions from a dynamo model based on principles of helicity conservation, discussed by Zhang et al. (2006). This model seems capable of explaining only a fraction of the regions with the wrong sign of the helicity. We attribute the remaining excess to additional current helicity production from the twisting of rising magnetic flux tubes, as suggested by Choudhuri et al. (2004a). We estimate the relative contributions of this effect and that connected with the model based on magnetic helicity conservation.

© 2006 WILEY-VCH Verlag GmbH & Co. KGaA, Weinheim

1 Introduction

According to the current consensus, the solar cycle is associated with the propagation of a magnetic-field wave, the “dynamo wave”, somewhere in the solar convective shell. The origin of this wave is dynamo action driven by the solar differential rotation and the helicity of turbulent convective flows, which drives the “ α -effect” formally introduced by Steenbeck, Krause, and Rädler in 1966 (see Krause & Rädler, 1980). This concept has been intensively discussed in the literature for about 50 years, beginning with the seminal paper of Parker (1955a) on the effects of cyclonic convection, and many important results have been obtained. Until recently however, the concept has remained to some extent speculative because no direct observations or laboratory confirmation of the key ingredient of the process, i.e. the α -effect, were available. In the last 12 years or so, observations of current helicity in solar active regions (Seehafer 1990; Pevtsov et al. 1994; Longcope et al. 1998; Zhang & Bao 1998, 1999) have presented a possibility of confronting theoretical ideas concerning the α -effect with observational evidence.

The point is that the α -effect consists of two contributions (Pouquet et al. 1976),

$$\alpha = \alpha^v + \alpha^m, \quad (1)$$

where α^v is determined by the mirror asymmetry of turbulence and is proportional to the hydrodynamic helicity $\chi^v = \langle \mathbf{v} \cdot \text{curl } \mathbf{v} \rangle$, while α^m is determined by the mirror asymmetry of the turbulent magnetic field and is proportional to the current helicity density $\chi^c = \langle \mathbf{j} \cdot \mathbf{b} \rangle$. Here \mathbf{v} is the turbulent convective velocity, \mathbf{b} is the small-scale magnetic field and $\mathbf{j} = \text{curl } \mathbf{b}$ is the corresponding electric current. $\langle \dots \rangle$ denotes averaging over an ensemble of convective pulsations. If the turbulent convection is considered as locally homogeneous and isotropic, χ^c is proportional to the magnetic helicity density $\chi^m = \langle \mathbf{a} \cdot \mathbf{b} \rangle$, where \mathbf{a} is the fluctuation of a magnetic vector-potential. Magnetic helicity is an integral of motion in a non-diffusive system and a topological invariant proportional to the linkage number of magnetic field lines.

Magnetic helicity is bounded from above by a value proportional to the magnetic energy (Moffatt 1978) and the capacity of the small-scale part of the magnetic spectrum is too small to allow an effective spectral transport of magnetic helicity. According to the conventional scenario, the solar dynamo begins from a state with a weak magnetic field with correspondingly small magnetic helicity. Because the large-scale magnetic field participating in the dynamo wave is helical, its magnetic helicity has to be compensated by the magnetic helicity (of opposite sign) of a small-scale magnetic field, which also contributes to α^m . Correspond-

* Corresponding author: sokoloff@dds.srcc.msu.su

© 2006 WILEY-VCH Verlag GmbH & Co. KGaA, Weinheim

ingly, magnetic helicity conservation effectively constrains the dynamo action.

On the other hand, proxies of χ^m can be determined from solar observations because the Zeeman effect as exploited observationally gives in principle three magnetic field components. In contrast, the Doppler effect used for velocity observations give the line-of-sight velocity only, and it is difficult to determine χ^v from observations (see however Komm et al. 2005).

Indeed, observations of χ^c in solar active regions provide the only direct observational (or experimental) information concerning the α -effect available at the moment. Note that a non-zero α -effect means that the electric current averaged over convective motions has a component parallel to the averaged magnetic field while the electric current in conventional electrodynamics is orthogonal to the magnetic field. This peculiar property of convection (or turbulence) in rotating electrically conductive flows obviously requires some observational or experimental confirmation.

Because the magnetic helicity data provide unique information concerning the key ingredient of the dynamo, making a comparison with predictions of dynamo theory is an attractive proposition. Such a comparison has been performed by Kleorin et al. (2003) and Zhang et al. (2006, hereafter Paper I) and shows that the data demonstrate something similar to the theoretical predictions. The discussions presented in these papers stress that the quality of both the data available and the theoretical models, as well as the length of the time series, are all rather limited and many obvious questions concerning the comparison remain obscure.

In particular, current helicity is observed at the solar surface while the dynamo action occurs somewhere inside the Sun. A magnetic tube rising to the solar surface to produce an active region can be twisted by the Coriolis force and so obtain a component of current helicity in addition to that generated in the solar interior. It means that the current helicity data exploited for comparison with dynamo theory could be biased by another contribution produced during the rise of the tube to the solar surface. Of course, the twist of magnetic tubes is interesting in itself in context of the theory of sunspots.

Note that the Coriolis force does not affect directly the magnetic and current helicities (i.e. the Coriolis force does not enter the equation for the evolution of the magnetic and current helicities). On the other hand, the Coriolis force creates the kinetic or hydrodynamic helicity in inhomogeneous turbulence, and the kinetic or hydrodynamic helicity enters the equation for the evolution of the magnetic and current helicities.

We stress that apart from the magnetic helicity conservation constraint in the solar dynamo, other possibilities for the production of current helicity production at the solar surface have been discussed (see e.g. Bao et al. 2002). In particular, Longscope et al. (1988) associated the current helicity with the twisting of a flux tube during the rise of the tube to the solar surface. A possible way to estimate the contribu-

tion to the current helicity connected with the tube rise was suggested by Choudhuri et al. (2004a). They considered the current helicity production during tube migration and predicted that this additional current helicity should dominate just at the beginning of the cycle. According to the theoretical predictions as well as the observational data, this contribution to the helicity follows a version of the sunspot polarity law, i.e. for the major part of the active region, the sign of current helicity in the northern solar hemisphere is opposite to that in the southern hemisphere. We stress that the polarity law predicts the behaviour of an average of the data, while substantial current helicity fluctuations are expected, which are important from the viewpoint of observations, theory and direct numerical simulations (this last conclusion is based on the work of Brandenburg & Sokoloff (2002). Choudhuri et al. (2004a) suggest that one effect of tube migration is to provide a substantial admixture of active regions which violate the polarity law just at the beginning of the cycle.

Note that Choudhuri et al. (2004a) defines a measure of helicity by using a measure of the twist in the magnetic field lines $\alpha = (\text{curl } \mathbf{B})_z / B_z$, see their Eq. (1) and corresponding explanation in the text of that paper. This definition differs from the standard definition and further clarification of this aspect of the model is desirable.

The aim of this paper is to compare the ideas presented in Choudhuri et al. (2004a) with the observational data for current helicity obtained at the Huairou Solar Observing station of the National Astronomical Observatories of China. We show that the available data is sufficient to demonstrate a contribution of the rise of flux tubes to the observed current helicity. According to our estimates about 20% of active regions at the beginning of the cycle have the "wrong" sign of current helicity due to this flux tube effect. On the other hand, the effect is rather moderate and localized in time, so that overall the current helicity data retain their role as a valuable source of information about the properties of current helicity in the domain of field generation.

2 Current helicity data for the beginning of the cycle

The first attempt to isolate the contribution from the rise of flux tubes from the current helicity data now available was undertaken in Paper I (see also Choudhuri et al. 2004b). Paper I concluded however that the current helicity observations studied in that paper do not allow the isolation of the effect of flux tube rise because the initial stage of the cycle was not covered by the observations available at that time.

The observational data used in our analysis were obtained at the Huairou Solar Observing station of the National Astronomical Observatories of China. The magnetograph using the FeI 5324 Å spectral line determines the magnetic field values at the level of the photosphere. The data are obtained using a CCD camera with 512×512 pixels over the whole magnetogram. The entire image size is

comparable with the size of an active region, which at about 2×10^8 m is comparable with the depth of the solar convective zone.

The observations are restricted to active regions on the solar surface and we obtain information concerning the surface magnetic field and helicity only. Monitoring of solar active regions while they are passing near the central meridian of the solar disc enables observers to determine the full surface magnetic field vector. The observed magnetic field is subjected to further analysis to determine the value $\nabla \times \mathbf{b}$. Because it is calculated from the surface magnetic field distribution, the only electric current component that can be calculated is $(\nabla \times \mathbf{b})_z$. As a consequence of these restrictions, the derived observable quantity is

$$H_c = \langle b_z (\nabla \times \mathbf{b})_z \rangle, \quad (2)$$

where x, y, z are local cartesian coordinates connected with a point on the solar surface, and the z -axis is normal to the surface.

Until now, the largest available systematic dataset for current helicity is that accumulated during 10 successive years (1988–1997) of observations of active regions, consisting of records of 422 active regions (Bao & Zhang 1998). It has been used for theoretical analysis and further data reduction by Kuzanyan et al. (2000), Zhang et al. (2002), Kleorin et al. (2003), Paper I and Kuzanyan et al. (2006).

The starting point of this paper is that we introduce new observational data into the discussion. The new data considered here covers the three years of the beginning of the solar cycle 23, namely 1998–2000. This dataset was discussed earlier by Bao et al. (2000, 2002), and contains data for 88 active regions¹. The new data are obtained by the same technique, and processed in much the same way, as the earlier dataset of Bao and Zhang (1998) covering the ten year period 1988–1997, see also Zhang and Bao (1998). Thus we feel it reasonable to merge these two sets of data and henceforth will consider them as a single continuous dataset for 510 active regions.

All of the available data is presented in Fig. 1. This figure shows the raw data concerning the sign of the helicity presented as a butterfly diagram. “+” denotes positive sign of helicity and dots negative. Two consecutive cycles are shown, and the distribution of signs more or less agrees with the polarity law. However a substantial number of active regions with the “wrong” sign of helicity can also be seen.

3 Active regions with the “wrong” sign of current helicity

Our aim in the following is to follow the dynamics of the fraction of the active regions with “wrong” sign of helicity,

¹ Note that Bao et al. (2000, 2002) were interested in comparing various observed quantities in addition to the current helicity. All the quantities were determined for 64 active regions only. Because we focus our attention on the current helicity, we use the whole dataset.

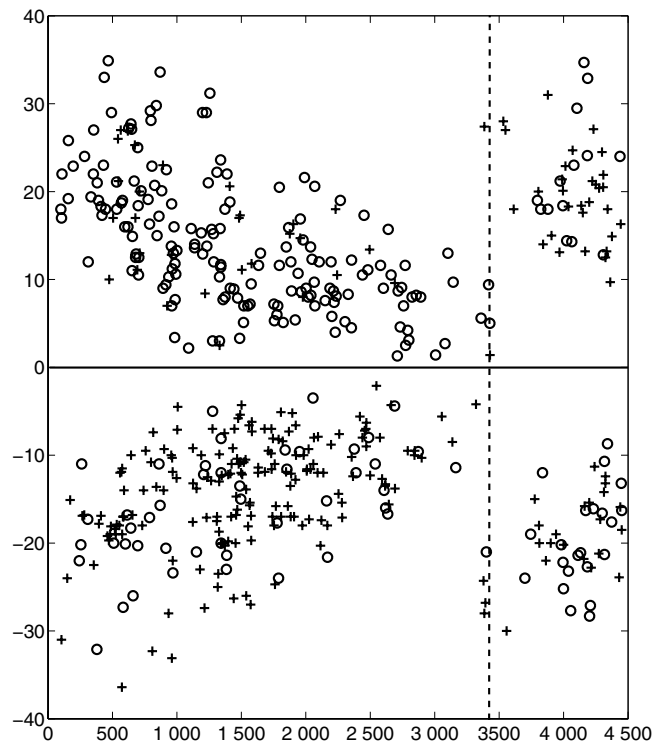


Fig. 1 Distribution of the sign of magnetic helicity from the observations at Huairou Solar Station at 1988–2000. Time in days from the beginning of observations is given on the horizontal axis, and latitude in degrees is given on the vertical axis. Signs “+” denote an active region with positive current helicity and circles denote the active region with negative current helicity. The vertical line separates the old dataset from the new.

as identified in the data presented in Fig. 1. In principle, the problem is nothing more than a straightforward calculation, comparing the two types of active region. A few practical points however have to be fixed.

The synthetic butterfly diagram. First of all, note that the observations cover an interval that is longer than the cycle length, and data from two activity cycles are included. The important point however is that no single cycle is covered completely and the most interesting part of the cycle, i.e. the beginning of the cycle, is known from one cycle, while the behaviour during the main part of the cycle is traced by the previous cycle. Thus we have to construct a synthetic cycle from the data.

The procedure used was as follows. We separated the data in the two cycles by a naked-eye decision. Because the cycle separation here is sufficiently pronounced we do not feel that anything more formal is required at the moment. We present the result of this procedure in Fig. 2.

Then we have to shift in time the data from the second cycle to place them at the beginning of the first cycle. The time-shift T has to be chosen to be equal to the cycle length, which is close to 11 yr, but is not known precisely *a priori*. We tried several values of T (see Fig. 3) and choose $T = 4000$ d (a value that is remarkably close to 11 years),

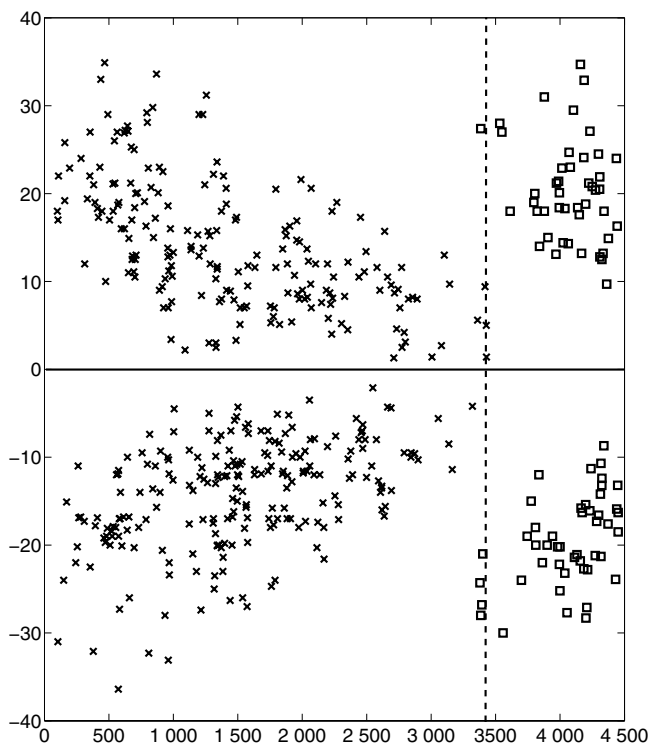


Fig. 2 Separation of the active regions with known current helicity over two consecutive cycles. Coordinates are as in Fig. 1. Crosses denote active regions of the first cycle, while the boxes indicate active regions from the second cycle.

based on a naked-eye estimate of the smoothness of the synthetic butterfly diagram. As a result, we arrive at the synthetic butterfly diagram shown in Fig. 4, where the signs of the current helicities are shown (again, plus signs denote positive helicity and circles negative).

The evolution of the sign of helicity in the synthetic cycle. Our aim in the following is to quantify the distribution shown in Fig. 4. The problem here is as follows. A conventional procedure would be to divide the temporal extent of the butterfly diagram into bins and calculate the relative number of regions with wrong sign (taking into account the polarity law and the hemisphere in which a given active region is located). The point however is that the data are quite noisy. If we choose a reasonable number of bins the number of active regions per bin drops substantially and the reliability of the results is low. Thus we use a trick well-known in statistics, but not so familiar in physics and astronomy. We calculate the cumulative number of active regions with the “wrong” sign of helicity as well as the total number of active regions from the beginning of the synthetic cycle (we are grateful to V. Tutubalin who suggested this procedure to us). This simple method substantially reduces the noise. We present the relative number of the active regions with the wrong sign of helicity in Table 1.

We conclude from Table 1 that active regions with the “wrong” sign of helicity occur preferentially at the beginning of the cycle, before cycle phase $t^* = 0.175$. Indeed,

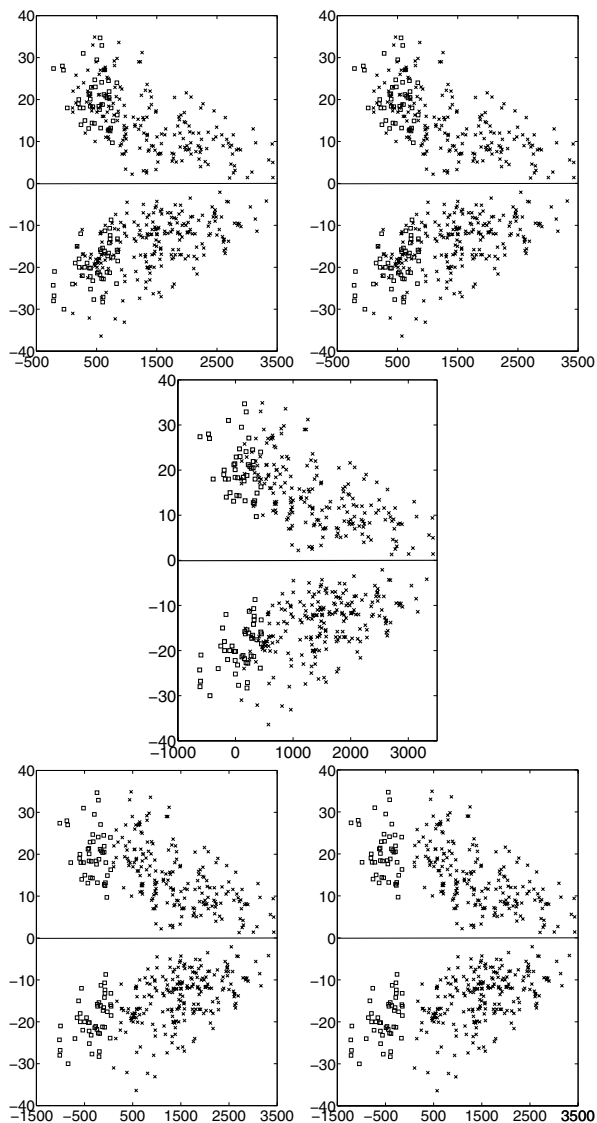


Fig. 3 Synthetic butterfly diagrams for various time-shifts T : $T = 3200$ days (top row, left); $T = 3600$ days (top row, right); $T = 4000$ days (middle row); $T = 4400$ days (bottom row, left); $T = 4600$ days (bottom row, right). A time-shift $T = 4000$ days (panel c) has been chosen as most plausible. Notation is as in Fig. 2.

for $t^* = 0.175$ we obtain $p = 54\%$ while $q \approx 24\%$ for all t^* in the Table. Note that the data before $t^* = 0.175$ come from the new set of observations introduced into the analysis in this paper. This is why we were unable to recognize this phenomenon in the analysis of Paper I.

An alternative interpretation of the data in Table 1 would be that the second cycle included in Table 1 is basically different from the first with respect to the polarity law for helicity, and that the new cycle contains more active regions with the wrong helicity sign than the previous. Although at the moment we do not see any reason to adopt this interpretation, we stress that publication of current helicity data from any additional year of observations would substantially con-

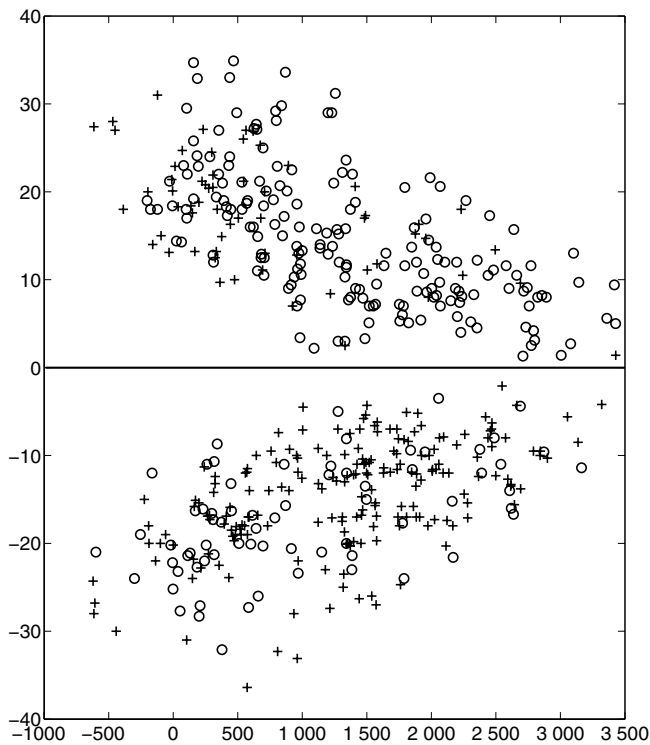


Fig. 4 Synthetic butterfly diagram with helicity signs. Notation is as in Fig. 1.

Table 1 Here t^* is the phase of the cycle, i.e. the fractional time from the beginning of the cycle; $t^* = 0$ corresponds to the beginning of the cycle and $t^* = 1$ to the end. n_- is the number of active regions with the wrong sign that occurs before phase T^* , while N_- means the number of active regions with the wrong helicity sign occurring after phase t^* . The corresponding notations for the active regions with the “correct” helicity sign are n_+ and N_+ . The relative numbers of the active regions before and after phase T^* are p and q respectively. The error bars are calculated as for the Poisson process.

| t^* | n_- | n_+ | p | N_- | N_+ | q |
|-------|-------|-------|--------------|-------|-------|--------------|
| 0.18 | 18 | 15 | $54 \pm 8\%$ | 112 | 364 | $24 \pm 2\%$ |
| 0.30 | 60 | 70 | $46 \pm 4\%$ | 70 | 309 | $18 \pm 2\%$ |
| 0.43 | 85 | 144 | $37 \pm 3\%$ | 45 | 235 | $16 \pm 2\%$ |
| 0.55 | 101 | 219 | $32 \pm 2\%$ | 31 | 160 | $15 \pm 3\%$ |
| 0.68 | 112 | 289 | $28 \pm 2\%$ | 18 | 90 | $17 \pm 4\%$ |
| 0.80 | 121 | 341 | $26 \pm 2\%$ | 9 | 38 | $19 \pm 5\%$ |

strain the possible interpretations. Neither do we see any reason to suggest that the observational data became much more noisy during the last two years of observations.

Note that the analysis above of the current helicity data differs from that undertaken in Paper I. That paper considered active regions with known rotation rate, and separated them into deep and shallow regions according to their rotation rate. A substantial number of the active regions observed have no reliable depth identification and were not included in the analysis. As a result, in Paper I we were unable to follow the temporal evolution of p and q in detail.

Here we do not separate the data by rotation rate/depth, but add some new data. As a result, we can follow the evolution of p and q , but must avoid discussion concerning the radial distribution of magnetic helicity.

4 Helicity conservation at the beginning of the cycle

The natural next step in our analysis is to decide to what extent the increased percentage of active regions with the “wrong” sign of helicity at the beginning of the cycle can be instructive for understanding physical processes within the Sun. We appreciate that the helicity data currently available are rather crude, and that any substantial improvement of the data probably lies in the quite remote future. Correspondingly, we restrict ourselves to the simplest theoretical models (which are in fact quite non-trivial) whose complexity is, we feel, more or less comparable with the state of the data. In particular, we consider the model suggested by Choudhuri et al. (2004a), alongside the model developed in Paper I, to examine the extent to which the models are compatible with the behaviour of the active regions with the “wrong” sign of helicity described above.

We stress that the physical mechanisms underlying these models are not mutually incompatible. However it is far from obvious how to combine them into a synthetic model. The point is that the model suggested by Choudhuri et al. (2004a) is based on the buoyancy of the magnetic flux tubes. Magnetic buoyancy applies (in the astrophysical literature) to two different situations (see Priest 1982). The first corresponds to a problem discussed by Parker (1966, 1979) and Gilman (1970) who considered a magnetic buoyancy instability of a stratified continuous magnetic field and did not use the magnetic flux tube concept. The other situation was considered by Parker (1955b), Spruit (1981), Spruit & van Ballegoijen (1982), Ferriz-Mas & Schüssler (1993), and Schüssler et al. (1994), who studied the buoyancy of discrete magnetic flux tubes. Paper I included effective velocities which can be considered as the small-scale magnetic buoyancy of the continuous mean magnetic field. Therefore, it is not clear at the moment how to combine the models by Choudhuri et al. (2004a) and Paper I into a synthetic model. In any case, we feel that such a step would be more than anything justified by the data now available.

Obviously, the model suggested by Choudhuri et al. (2004a) which focusses attention on the migration of flux tubes to the solar surface broadly explains the behaviour under discussion. Note however that the simulated butterfly diagram for the sign of current helicity suggested by Choudhuri et al. (2004b) looks exaggerated, because the active regions with the “wrong” sign are obviously dominant at the beginning of the cycle. The maximal corresponding index from Table 1 is $p = 54\% \pm 8\%$ only. The question is to what extent the model of Choudhuri et al. (2004a) can explain the other features of the observed helicity distribution

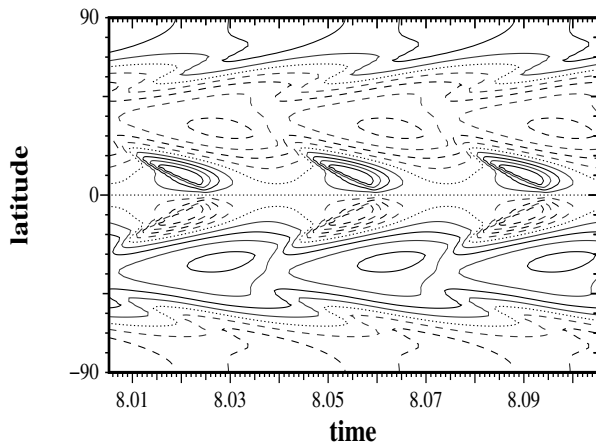


Fig. 5 Artificial butterfly diagram for the current helicity obtained by combining diagrams from deep and shallow domains. Contours of positive values are shown as solid curves, negative values are broken, and the zero contour is dotted.

investigated by Kleerorin et al. (2003) and Paper I. However, such a study is beyond the scope of this paper.

We use below a two-dimensional axisymmetric nonlinear dynamo model which includes an explicit radial coordinate, and takes into account the curvature of the convective shell and density stratification. The nonlinear model takes into account algebraic quenching of the total α -effect and turbulent magnetic diffusivity. We split the total α -effect into its hydrodynamic and magnetic parts. The calculation of the magnetic part of the α effect is based on the idea of magnetic helicity conservation and the link between current and magnetic helicities. In the model we use a dynamical equation for magnetic helicity which includes production, transport (helicity fluxes) and molecular dissipation of magnetic helicity (see Paper I for details).

The model of Paper I, based on magnetic helicity conservation, does not appear in principle incompatible with the data (here and below we use the model suggested by Paper I without modification). We demonstrate this by the following simple experiment. We take two butterfly diagrams, for the deep and shallow domains of the model of Paper I, for some particular choice of parameters and formally combine them with an arbitrary weighting. For example, we show in Fig. 4 the result from combining a “deep” butterfly diagram (Fig. 6 of Paper I, weighted at 0.8), with a surface diagram (Fig. 7 of Paper I with weight 0.2). This figure looks quite similar to the data from Table 1, and as convincing as the plot presented in Choudhuri et al. (2004b). We stress however that physically the contributions from the deep and shallow domains cannot be arbitrarily combined as independent contributions to a butterfly diagram, and a deeper analysis is required.

Analysis of the data obtained from a dynamo model computed as in Paper I for a quite typical set of values of the governing parameters proceeds as follows. (Specifically, the model has the dynamo number $D = C_\alpha C_\omega$ with $C_\alpha = -5$

Table 2 Relative cumulative volumes occupied by the current helicity with the “wrong” sign: i_- – before the phase t^* , n_- – after the phase t^* . The data are given separately for the lower domain of the computation box ($0.64 < r < 0.80$) and the whole radial extent of the computational box ($0.64 < r < 1$).

| t^* | $0.64 < r < 0.80$ | | $0.64 < r < 1$ | |
|-------|-------------------|-------|----------------|-------|
| | i_- | n_- | i_- | n_- |
| 0.18 | 20 % | 15 % | 6 % | 5 % |
| 0.30 | 17 % | 16 % | 5 % | 5 % |
| 0.42 | 14 % | 19 % | 4 % | 6 % |
| 0.55 | 13 % | 28 % | 4 % | 10 % |
| 0.68 | 14 % | 40 % | 4 % | 15 % |
| 0.80 | 15 % | 56 % | 5 % | 21 % |

and $C_\omega = 6 \times 10^4$, the relaxation time of the magnetic helicity varies between 5 and 5×10^4 from top to bottom of the convection zone, and the density parameter $a = 0.3$. Further details can be found in Paper I.) From the solution in the computational box defined by radial (r), co-latitude (θ) and time (t) coordinates, we identify a domain associated with a particular activity wave. We performed this identification based on common sense arguments and naked-eye estimates. We tried several prescriptions for this separation of the data. Because the overlapping of the activity waves in the simulated (as well as observed) butterfly diagrams is quite modest, the results seem quite robust with respect to the particular choice of separation procedure. We omit here presentation of a set of rather similar tables, but recognize that a more systematic method of separation of the data would be highly desirable.

Following Paper I, we identify the the relative number of the active regions possessing the “wrong” sign of current helicity with the relative volume of the computational box possessing the “wrong” helicity sign. More precisely, we introduce the value $i_-(t^*)$ as a relative volume of the computational box with the “wrong” sign of the current helicity, up to cycle phase t^* , while n_- is the relative volume of the computational box with the wrong sign after phase t^* .

Of course, the values i_- (to be compared with p from Table 1) and n_- (to be compared with q from Table 1) depend on the governing parameters of our model, but the general shape of the behaviour seems to be quite robust. More details concerning the computation of i_- and n_- are given in Paper I. The maximal values of i_- are about 20%. We present typical values of i_- and n_- in Table 2.

We see from this Table that the behaviour of i_- is quite different from that of p , e.g. p decreases with t^* . We were able to find governing parameters which gives some decay of i_- at the beginning of the cycle but i_- then increases at the end of the cycle. In addition, the typical values of i_- are substantially lower than those for p . Note that i_- becomes larger in the lower domain of the computational box ($0.64 < r < 0.80$). The values of i_- become much smaller if the whole computational box is considered ($0.64 < r < 1$).

The results for n_- are naturally connected with those for i_- .

We conclude from this comparison that our model based on the magnetic helicity conservation cannot by itself reproduce details of the behaviour of the index p just at the beginning of the cycle. In the context of our modelling, this behaviour must be attributed to the additional current helicity produced by the rise of flux tubes to the solar surface. Of course, we have not shown that this conclusion applies to all possible dynamo models!

5 Results and discussion

We conclude from the above analysis, from comparison with the model of Paper I, that the current helicity data from solar active regions are consistent with a clear contribution from the helicity production during the rise of magnetic flux tubes to the solar surface in the formation of active regions. Based on the data available and theoretical modelling we can give an order-of-magnitude estimate for the various contributions to the sign of the surface helicity. About 15% of the cases with helicity of the "wrong" sign can be attributed to helicity of the "wrong" sign originating in the generation domain (this figure is obtained from Table 2 as a typical value for i_-). About 20%-30% of the cases with the "wrong" helicity sign must be attributed to the processes associated with the flux tube rise (estimated as a difference between maximal and minimal values of p) and the remainder, about 10%, is attributed to observational noise.

The idea that the twisting of rising magnetic flux tubes leads to the effect being discussed looks interesting and promising in the context of the physics of active regions. From the viewpoint of solar dynamo theory the effect appears as a bias, but its role is limited to the beginning of the cycle, and is rather modest. The current helicity data retains its importance as a unique source of information about the solar α -effect. Taking into account that the domain of field generation is spatially separated from the region observed, and also other observational problems (see details in Kleerorin et al. 2003 and Paper I), the current helicity data seem to be surprisingly useful for comparison with theoretical interpretations.

Our analysis in this paper is not directed towards an investigation of the radial location of the generation domain. Our results do however support the localization of the domain deep inside the convective shell (cf. left and right hand columns of Table 2; the mechanism of Choudhuri et al. (2004a) is also associated with a deep location of the generation domain).

In spite of the obvious role of twisting processes, magnetic helicity conservation appear to be responsible for a substantial fraction of the active regions with the "wrong" sign of helicity. In particular, we note that an increase of q at the very end of the cycle (Table 1) might be compared with the growth of i_- at the end of the cycle (Table 2).

Note that the tendency of the sign of current helicity to reverse at the beginning of solar cycle was mentioned by Hagino & Sakurai (2005), from current helicity data obtained at the Solar Flare Telescope at Mitaka and the Solar 65-cm telescope at Okayama. The time variation of the sign of current helicity was inferred from the vector magnetograms observed at the solar surface. They connected this phenomenon with the inherent properties of the twisted magnetic field originating from the solar subatmosphere. An opposing interpretation was suggested by Pevtsov et al. (2001) who attributed the tendency to an observational effect caused by Faraday rotation (see however the analysis of Bao et al. 2000). We appreciate that the problem needs further clarification and believe that a systematic comparison of the data obtained by various observational groups can provide a crucial contribution towards this end.

We stress again the preliminary nature of our findings. Our results are constrained by the limited extent and quality of the available observational data as well as by the limited understanding of the role of current helicity in solar activity at the moment. Whilst recognizing that future progress in theory and observations may well lead to a revision of our conclusions, we nevertheless believe that the results above can stimulate progress in the problem and, in particular, can provide real constraints for theories of the solar cycle.

Acknowledgements. The research was supported by grants 10233050, 10228307, 10311120115 and 10473016 of the National Natural Science Foundation of China, and TG 2000078401 of the National Basic Research Program of China. DS and KK are grateful for support from the Chinese Academy of Sciences and NSFC towards their visits to Beijing, as well as RFBR-NNSFC 02-02-39027 and 05-02-39017. KK would also like to acknowledge support from RFBR, grants 03-02-16384 and 05-02-16090. DS is grateful for financial support from INTAS by grant 03-51-5807 and RFBR by grant 04-02-16068.

References

- Bao, S.D., Ai, G.X., Zhang, H.Q.: 2002, in: H. Rickman (ed.), *Highlights of Astronomy*, Vol. 12, San Francisco, p. 392
- Bao, S.D., Ai, G.X., Zhang, H.Q.: 2000, *JApA* 21, 303
- Bao, S.D., Sakurai, S.D., Suemitsu, Y.: 2002, *ApJ* 573, 445
- Bao, S.D., Zhang, H.Q.: 1998, *ApJ* 496, L43
- Brandenburg, A., Sokoloff, D.: 2003, *GApFD* 96, 319
- Choudhuri, A.R., Chatterjee, P., Nandy, D.: 2004a, *ApJ* 615, L57
- Choudhuri, A.R., Chatterjee, P., Nandy, D.: 2004b, in: A. Stepanov, E. Benevolenskaya, A. Kosovichev (eds), *Multi-Wavelength Investigations of Solar Activity*, IAU Symp. No. 223, Cambridge University Press, p. 45
- Ferriz-Mas, A., Schüssler, M.: 1993, *GApFD* 72, 209
- Gilman, P.A.: 1970, *ApJ* 162, 1019
- Hagino M., Sakurai T.: 2005, *PASJ* 57, 481
- Kleerorin, N., Kuzanyan, K., Moss, D., Rogachevskii, I., Sokoloff, D., Zhang, H.: 2003, *A&A* 409, 1097
- Komm, R., Howe, R., Hill, F., González, H.I., Toner, C.: 2005, *ApJ* 630, 1184
- Krause, F., Rädler, K.-H.: 1980, *Mean-Field Magnetohydrodynamics and Dynamo Theory*, Pergamon, Oxford
- Kuzanyan, K.M., Bao S., Zhang, H.: 2000, *Solar Phys.* 191, 231

- Kuzanyan, K.M., Pipin, V., Seehafer, N.: 2006, *Solar Phys.* 233, 185
- Longcope, D.W., Fisher, G.H., Pevtsov, A.A.: 1998, *ApJ* 507, 417
- Moffatt, H.K.: 1978, *Magnetic Field Generation in Electrically Conducting Fluids*, Cambridge University Press, New York
- Parker, E.: 1955a, *ApJ* 122, 293
- Parker, E.: 1955b, *ApJ* 121, 491
- Parker, E.: 1966, *ApJ* 145, 811
- Parker, E.: 1979, *Cosmical Magnetic Fields*, Clarendon, Oxford
- Pevtsov A.A., Canfield R.C., Latushko S.M.: 2001, *ApJ* 549, L261
- Pevtsov, A.A., Canfield, R.C., Metchalf, T.R.: 1994, *ApJ* 425, L117
- Pouquet, A., Frisch, U., Leorat, J.: 1976, *JFM* 77, 321
- Priest, E.R.: 1982, *Solar Magnetohydrodynamics*, D. Reidel Publ. Co., Dordrecht
- Seehafer, N.: 1990, *SoPh* 125, 219
- Schüssler, M.: 1981, *A&A* 94, 17
- Schüssler, M., Caligari, P., Ferriz-Mas, A., Moreno-Insertis, F.: 1994, *A&A* 281, L69
- Spruit, H. C.: 1981, *A&A* 98, 155
- Spruit, H. C., van Ballegoijen, A. A.: 1982, *A&A* 106, 58
- Zhang, H., Bao, S.: 1998, *A&A* 339, 880
- Zhang, H., Bao, S.: 1999, *ApJ* 519, 876
- Zhang H., Bao S., Kuzanyan K. M.: 2002, *ARep* 46, 414
- Zhang, H., Sokoloff, D., Rogachevskii, I., Moss, D., Lamburt, V., Kuzanyan, K., Kleorin, N.: 2006, *MNRAS* 365, 276 (Paper I)